

MHD WAVES IN THE NEIGHBOURHOOD OF A 2D X-TYPE NEUTRAL POINT

J. A. McLaughlin and A. W. Hood

Mathematical Institute, University of St Andrews, St Andrews, KY16 9SS, Scotland

ABSTRACT

A linear, fast magnetoacoustic wave is generated at a boundary and travels towards an magnetic X-type neutral point. Due to refraction, the wave wraps itself around the null point, causing a large current to accumulate there. Simulations show that the current build up is exponential in time. The numerical simulations are in good agreement with analytic work based on a WKB solution obtained by the method of characteristics.

Key words: Sun; Refraction; Magnetoacoustic waves.

1. INTRODUCTION

Magnetic reconnection is considered to be of fundamental importance in many astrophysical phenomena and its role in coronal heating has been widely investigated (Priest & Forbes, 2000). In such studies, the importance of the null points of the magnetic field is often highlighted, (Birn, Hesse & Schindler, 1989; Lau & Finn, 1991; Greene, 1993; Craig & Henton, 1995; Craig & Fabling, 1996). Thus, an essential question to ask is how do external disturbances behave in the neighbourhood of such neutral points? Much work has been done on the properties of two-dimensional and three-dimensional null points, their reaction to boundary perturbations and their subsequent collapse (Craig & McClymont, 1993; Parnell *et al*, 1996; Rickard & Titov, 1996; Priest & Titov, 1996; Mellor, Titov & Priest, 2002). This investigation resembles that of Galsgaard, Priest and Titov (2003). Rather than study the collapse of null points, here we investigate the behaviour of a fast magnetoacoustic wave as it propagates into the vicinity of a two-dimensional X-type neutral point. The different sections of this poster summaries some important points of this study.

2. BASIC EQUATIONS AND NUMERICAL SETUP

We solve the two-dimensional induction and momentum equations for a low β plasma with a high magnetic Reynolds number, where we consider length-scales much less than the scale-height. We impose a simple potential

X-point magnetic field as our equilibrium, as illustrated in Figure 1, and perturb the system. The resulting linearised, perturbation equations are then solved numerically using a two-step Lax-Wendroff scheme. We initially

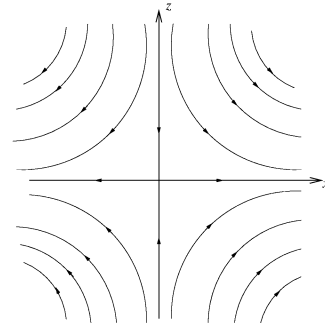


Figure 1. Our choice of equilibrium magnetic field.

consider a box with a single wave coming in from the top boundary. We set up the boundary conditions such that the first derivatives of the perpendicular velocity are zero there, although tests show that the central behaviour is unaffected by these choices. The other boundary conditions follow from the remaining equations and the solenoidal condition, $\nabla \cdot \mathbf{B} = 0$.

In our model, we have neglected gas pressure and imposed no velocity in the y -direction. Thus, we only consider fast magnetoacoustic waves.

Our linearised, perturbation equations are:

$$\begin{aligned} \frac{\partial \sigma}{\partial t} &= v_A^2(x, z) \left(\frac{\partial b_z}{\partial x} - \frac{\partial b_x}{\partial z} \right), \\ \frac{\partial b_x}{\partial t} &= -\frac{\partial \sigma}{\partial z}, \quad \frac{\partial b_z}{\partial t} = \frac{\partial \sigma}{\partial x}, \end{aligned}$$

where the Alfvén speed, $v_A(x, z) = \sqrt{x^2 + z^2}$, σ is closely linked to the perpendicular velocity ($\sigma = -|\mathbf{B}_0|v_\perp$, where \mathbf{B}_0 is our dimensionless equilibrium magnetic field) and b_x and b_z are components of the perturbed magnetic field.

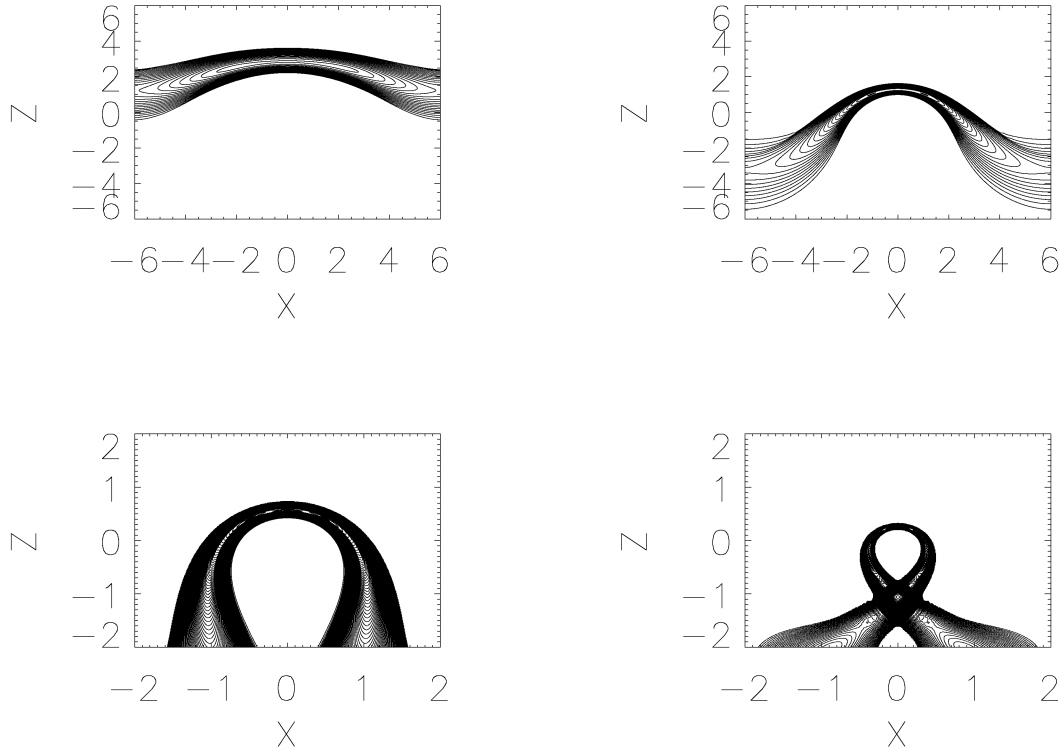


Figure 2. Contours of a fast wave sent in from upper boundary and its resultant propagation at times (a) $t=1.0$ units, (b) $t=1.8$ units, (c) $t=2.6$ units and (d) $t=3.4$ units. The axes have been scaled down in these lower two subfigures to draw attention to the central behaviour.

3. RESULTS

The linear, fast magnetoacoustic wave travels into the neighbourhood of the X-point and bends around it. Since the Alfvén speed ($v_A(x, z)$) is spatially varying, different parts of the wave travel at different speeds, and it travels faster the further it is away from the origin. So due to refraction, the wave wraps around the null point, as shown in figure 2. A similar phenomenon was found by Nakariakov and Roberts (1995).

Since the Alfvén speed drops to zero at the null point, the wave never reaches there, but the length scales rapidly decrease indicating that the current (and all other gradients) will increase. Consider the wavefront at $x = 0$. Here the vertical velocity is $v_z = \frac{dz}{dt} = -z$. Thus, the start of the wave is located at a position $z_s = 6e^{-t}$, when the wave is initially at $z = 6$. If the end of the wave leaves $z = 6$ at $t = t_0$ then the location of the end of the wave is $z_e = 6e^{t_0-t}$. The distance between the front and end of the wave is $\delta z = 6(e^{t_0} - 1)e^{-t}$ and this decreases with time, suggesting that all gradients will increase exponentially.

4. ANALYTICAL WORK

Substituting $\sigma = e^{i\phi(x,z)} \cdot e^{-i\omega t}$ into our wave equation $\frac{\partial^2 \sigma}{\partial t^2} = (x^2 + z^2) \left(\frac{\partial^2 \sigma}{\partial x^2} + \frac{\partial^2 \sigma}{\partial z^2} \right)$ and assuming that $\omega \gg 1$ (WKB approximation), leads to a first order PDE of the form $\mathcal{F}(x, z, \phi, \frac{\partial \phi}{\partial x}, \frac{\partial \phi}{\partial z})$. Applying the method of characteristics, we generate the solution

$$\begin{aligned} \phi &= -\omega^2 s \\ x &= \left[x_0 \cos\left(\frac{Ax_0}{6}s\right) + 6 \sin\left(\frac{Ax_0}{6}s\right) \right] e^{-As} \\ z &= \left[6 \cos\left(\frac{Ax_0}{6}s\right) - x_0 \sin\left(\frac{Ax_0}{6}s\right) \right] e^{-As} \end{aligned}$$

where s is some parameter along the characteristic and x_0 is a starting point distinguishing between different characteristic curves. Figure 3 shows constant ϕ at four different values of the parameter s . s is comparable to t and so the subfigures below can be directly compared to figure 2. The agreement between the analytic model and the leading edge of the wavefront is very good, as seen in an overplot of a contour and our WKB solution in figure 4. Note that there is a difference between the boundary conditions of the simulations and the analytical model.

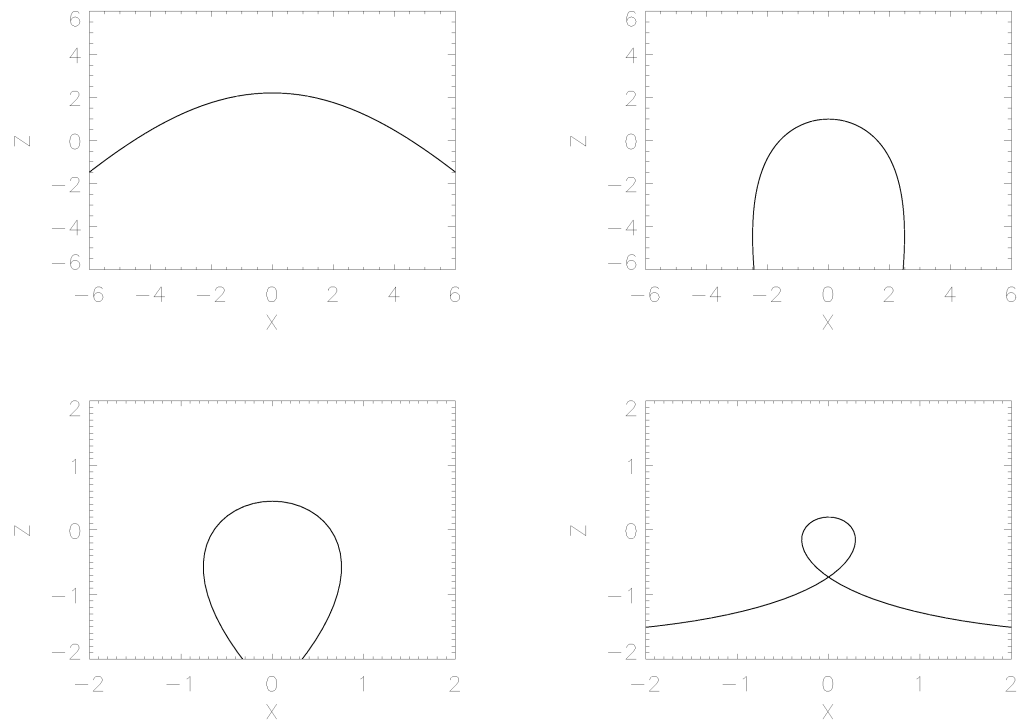


Figure 3. Plots of WKB solution for a wave sent in from upper boundary and its resultant propagation at times (a) $s=4$, (b) $s=8$, (c) $s=12$ and (d) $s=16$. Note the axes change in (c) and (d).

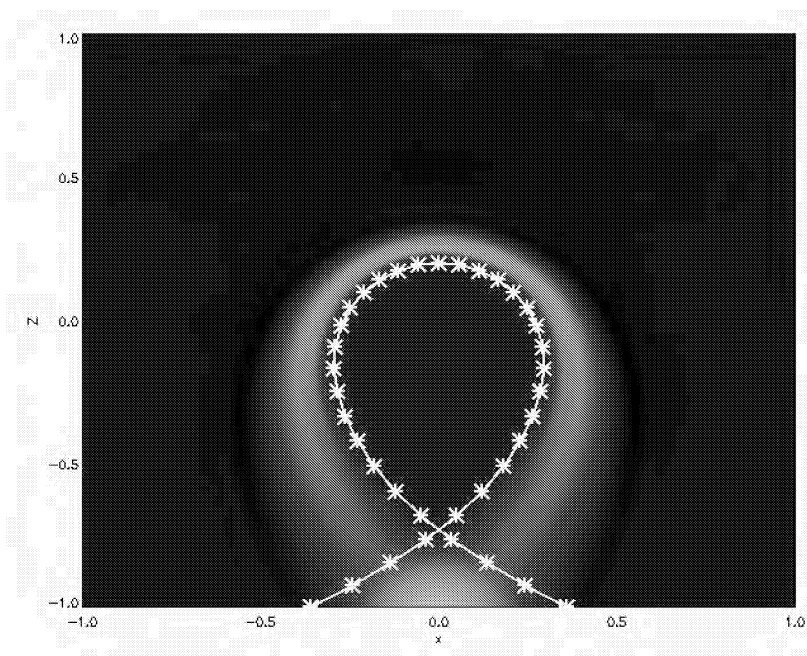


Figure 4. Comparison of numerical simulation and analytical solution at time $t=3.4$ units.

5. CURRENT

Since we have a changing perturbed magnetic field whose gradients are increasing in time, we have a build up of current density. Simulations show that there is a large current accumulation at the neutral point (Figure 5) and that this build up is exponential in time (Figure 6), in keeping with our discussion on the thickness of the wave pulse.

6. CONCLUSIONS

These proceedings describe the start of an investigation into the nature of MHD waves in the neighbourhood of null points. From the work explained above, it has been seen that when a fast magnetoacoustic wave propagates near a magnetic X-type neutral point, the wave wraps itself around the null point due to refraction (at least in two dimensions). It has also been seen that this behaviour causes a large current density to accumulate at the null and simulations have shown that this build up is exponential, although the exponential behaviour is probably due to the linearization of the problem. However, it is clear this refraction of the wave focusses the energy of the incident wave towards the null point. As seen from both the numerical work and analytical approximations, the wave continues to wrap around the null point, again and again. The physical significance of this is that any disturbance in the neighbourhood of a neutral point in the solar corona will be drawn towards the region of zero magnetic field and focus all of its energy at this point. Hence, this is where the build up of current will occur and energy will be dissipated. Thus, null points should effectively trap and dissipate the energy contained in fast magnetoacoustic waves. It is expected that these are locations of energy deposition and preferential heating.

REFERENCES

- Birn, J., Hesse, M. and Schindler, K. (1989) Filamentary structure of a three-dimensional plasmoid, *JGR*, **94**, 241-251
- Craig, I. J. D. and Fabling, R. B. (1996) Exact Solutions for Steady State, Spine, and Fan Magnetic Reconnection, *ApJ*, **462**, 969-
- Craig, I. J. D. and Henton, S. M. (1995) Exact Solutions for Steady State Incompressible Magnetic Reconnection, *ApJ*, **450**, 280-
- Craig, I. J. D. and McClymont, A. N. (1993) Linear theory of fast reconnection at an X-type neutral point, *ApJ*, **405**, 207-215
- Craig, I. J. D. and McClymont, A. N. (1991) Dynamic magnetic reconnection at an X-type neutral point, *ApJ*, **371**
- Galsgaard, K., Priest, E. R. and Titov, V. S. (2003) Numerical experiments on wave propagation towards a 3D null point due to rotational motions, *JGR*, **108**, Issue A1
- Greene, J. M. (1993) Reconnection of vorticity lines and magnetic lines, *Phys. Fluids B* **5**, 2355-2362
- Lau, Y. and Finn, J. M. (1991) Three-dimensional kinematic reconnection of plasmoids, *ApJ*, **366**, 577-591
- Mellor, C., Priest, E. R. and Titov, V. S. (2002) Exact Solutions for Spine Reconnective Magnetic Annihilation, *J Plasma Phys.*, **68**, 221-235
- Nakariakov, V. M. and Roberts, B. (1995) On Fast Magnetosonic Coronal Pulsations, *Solar Physics*, **159**, 399-402
- Parnell, C. E., Smith, J., Neukirch, T. and Priest, E. R. (1996) The structure of three-dimensional magnetic neutral points, *Phys. Plasmas*, **3**, 759-770
- Priest, E. R., 1982, *Solar Magnetohydrodynamics*, D. Reidel publishing Company
- Priest, E. R. and Forbes, T., 2000, *Magnetic Reconnection*, Cambridge University Press
- Priest, E. R. and Titov, V. S. (1996) Magnetic Reconnection at three-dimensional null points, *Phil. Trans. Roy. Soc. Lond. A*, **354**, 2951-2992
- Rickard, G. J. and Titov, V. S. (1996) Current Accumulation at a Three-dimensional Magnetic Null, *ApJ*, **472**, 840-852

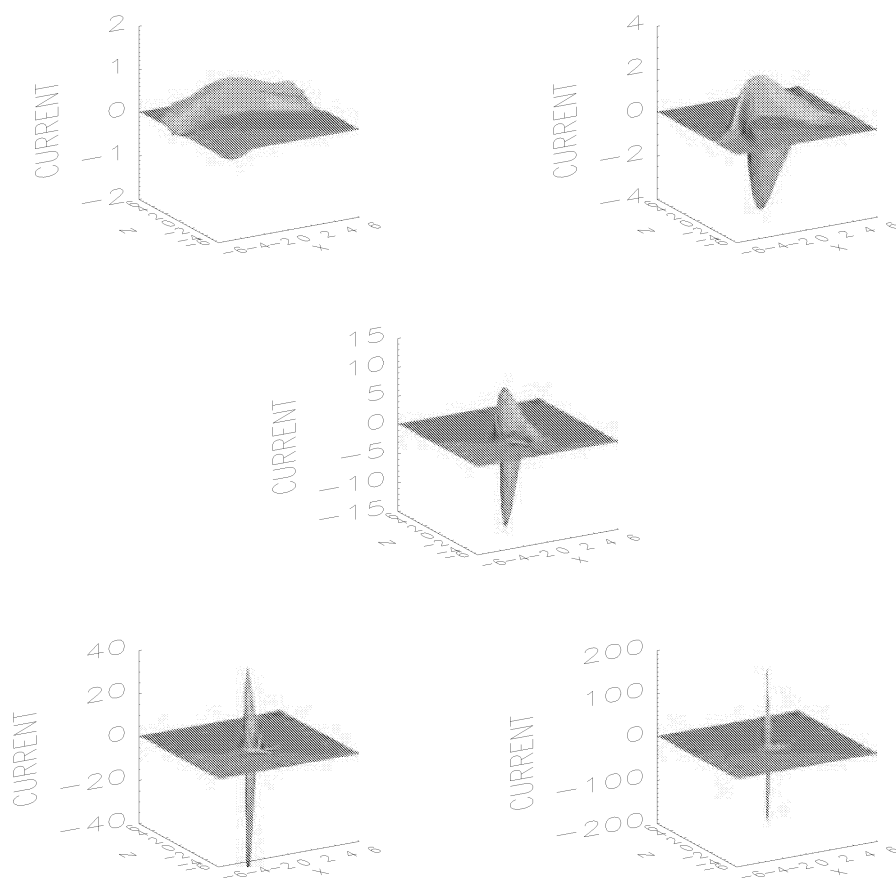


Figure 5. Shaded surfaces showing the build up of current at times (a) $t=1.0$, (b) $t=1.8$, (c) $t=2.6$, (d) $t=3.4$ and (e) $t=4.2$

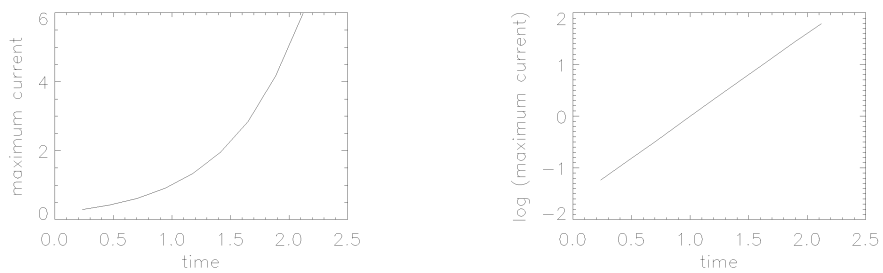


Figure 6. Maximum current against time elapsed (left), log maximum current against time elapsed (right)